Received: 27 September 2024 | Revised: 22 January 2025 | Accepted: 28 January 2025

IET Generation, Transmission & Distribution

DOI: 10.1049/gtd2.70021

The Institution of Engineering and Technology WILEY

ORIGINAL RESEARCH

Virtual power line control for interlinking converters on AC, DC and hybrid grid links

Julen Paniagua | Eneko Unamuno | Jon Andoni Barrena

Faculty of Engineering, Mondragon Unibertsitatea, Mondragon, Spain

Correspondence
Julen Paniagua, Faculty of Engineering, Mondragon Unibertsitatea, Loramendi 4, 20500 Mondragon, Spain.
Email: jpaniagua@mondragon.edu

Funding information
Eusko Jaurlaritza, Grant/Award Numbers: EP4H2 (KK-2022/00039), RESINET (KK-2023/00042)

Abstract

The increasing integration of renewable energy sources is making power systems evolve, driving the necessity to interconnect different power systems to improve the robustness and operation of grids. Here, the so-called virtual power line (VPL) control for interlinking converters (ICs) is presented, whose purpose is to couple different electric systems analogously to a classical transmission line. The VPL control employs local measurements, and it does not require any communication link to operate. Two VPL control variants are presented: the dual grid-supporting VPL control and the single grid-forming VPL (SGF-VPL) control. Both support the frequency and/or voltage of the interconnected grids, and the latter provides grid-forming capabilities for one of the interconnected systems. The performance of VPL controllers show how the frequency and voltage nadir values are improved by 36% (when comparing low and strong coupling results), while the rate of change of frequency and voltage can be decreased by 49.6%, with a 40% faster settling time. Furthermore, it is demonstrated how the SGF-VPL is able to set the grid when other grid-forming units fail, and the flow of power happens naturally through ICs from generation to consumption areas as if all devices were part of the same electric system.

1 | INTRODUCTION

The growing trend of the global energy consumption, the concern about environmental issues and the objective of being energetically self-sufficient are driving the electric power generation toward a renewable energy source (RES)-based model [1]. In this transition, many fossil fuel power plants are being replaced by photovoltaic (PV) or wind power (WP) plants. This fact entails the substitution of traditional powerful synchronous generators (SG) by converter-interfaced ones. By doing so, the total mechanical inertia of power systems is being reduced, leading to system weakening and instability issues under sudden load variations [2–4], if no actions are taken to actively support the power systems through newly installed grid-connected converter controls [5].

Most of the aforementioned RES require a dc stage on their power conversion process, and considering the advantages that dc operation offers in power conversion and transmission [6, 7], dc power systems are becoming very popular at different scales and applications. Furthermore, many energy storage systems (ESSs) employ dc voltage in their operation, so their connection to dc power systems is simpler, where the energy coming from different RES can be managed locally [8].

The future power system scenario is therefore envisioned to comprise subgrids of different natures, frequencies, and/or voltage levels, where in some cases grids cannot be directly interconnected as it is done when power systems of similar characteristics are tied. However, these interconnections can be carried out with different types of power electronic converters, also known as interlinking converters (ICs) [9]. In addition to controlling the flow of power between interconnected subgrids, ICs can be controlled to offer a wide variety of services to improve the performance of the system [10].

Traditional power system tying methods (i.e., power lines or transformers) offer very interesting features to interconnect synchronised ac systems and dc systems of the same voltage. The most relevant advantage is that they couple the interconnected grids in terms of inertial (transient) and primary (steady-state) responses. This means that under load and generation variations, all the grid-connected generators respond

TABLE 1 Summary of IC controls at the scope of proposed the virtual power line (VPL) control.

Ref.	Year	Link type	Proportional power sharing	Per-unit equalisation	Transient support	GF capability
[11]	2013	ac-dc μG	✓	✓	✗	✗
[12]	2016	dc-dc nG	✓	✓	✗	✗
[13]	2017	ac-ac μG	✓	✓	✗	✗
[14]	2022	ac-dc μG	✓	✓	✗	✗
[15]	2015	ac-dc μG	✓	✓	✗	✗
[16]	2019	dc-dc μG	✓	✓	✗	✗
[17]	2017	ac-dc μG	✓	✓	✗	✗
[18]	2017	ac-dc μG	✓	✓	✗	✗
[19]	2021	ac-dc μG	✗	✓	✗	✗
[20]	2021	ac-ac Trans.	✓	✗	✓	✗
[21]	2022	ac-dc μG	✗	✗	✓	✗
[22]	2024	ac-dc μG	✗	✗	✓	✓
[23]	2024	ac-ac Trans.	✓	✓	(✓)	✓
[24]	2022	ac-dc μG	✓	✓	✗	✗
VPL	–	any	✓	✓	✓	✓

Abbreviation: GF, grid-forming.

to keep the voltage and frequency stable. In addition, a very meshed grid provides more paths for the power to flow, significantly increasing the power transmission capability and the reliability of the system. Last but not least, when a power line is employed in an interconnection, it implies the extension of the grid to another area, setting the voltage and/or frequency at the interconnection node. If this aspect is analysed from a grid-connected converter control perspective, a power line works as a grid-forming (GF) unit for the new area, where no other GF unit is mandatory to operate the grid.

Among the interlinking converter (IC) controls already proposed in the literature, to the best of the authors' knowledge, none of the existing techniques replicate the above-mentioned characteristics and extend them to hybrid ac/dc, non-synchronised ac, or dc interconnections of different voltage levels. For the sake of clarity, the literature revision gathering the comparable controls with the VPL is summarised in Table 1.

Firstly, IC controls that do not consider transient support coupling between interconnected grids, but instead focus on grid equalisation and power sharing, are identified. Proposals in references [11–14] use proportional-integral controllers to equalise the per-unit values of frequency and voltage (for ac and dc grids, respectively) at interconnected grids by exchanging active power among them. Similarly, in reference [15], the per-unit errors of a hybrid microgrid are equalised and the authors also include the effect of secondary and tertiary controls. In reference [16], Shi et al. apply the *virtual transformer* philosophy on a dc-dc link, but instead of using a per-unit value to equalise the voltages of the interconnected grids, a constant voltage proportion is used to perform the power exchange. In reference [17], the authors propose a proportional power-sharing technique in which, instead of using the IC terminal measurements, the common voltages of the ac and dc subsystems are estimated to achieve better active and reactive power sharing. One of the main drawbacks of the aforementioned control is that it requires knowing the structure and parameters of the interconnected systems. With similar characteristics, Mortezapour et al. propose an IC control in reference [18] that uses predefined control indices to achieve correct power sharing according to the power capacity of interconnected ac and dc microgrids.

Second, the control strategies that apart from sharing power between grids aim to provide transient support have been classified. According to the authors, the IC control for hybrid ac/dc microgrids in reference [19] contributes to the power sharing among the different resources of interconnected systems, achieving zero frequency deviation at the ac side frequency and tighter voltage deviation at the dc side when comparing to conventional $P-V$ control method. Apart from that, this strategy employs the dc bus voltage derivative to achieve a smooth overshoot-free response of the IC. However, this limitation does not enable the equalisation of interconnected grids or the coupling and improvement of the transient response of both interconnected systems. The strategy in reference [20] proposes a coordinated frequency regulation for asynchronous ac grids tied through a high-voltage dc (HVDC) multi-terminal grid, which combines droop, inertia-emulation and a frequency safety algorithm. This technique improves the transient response of ac grids, extracting power from adjacent grids. The p.u. equalisation of systems is not achieved, and transient support is not provided in either ways of the interconnection. Authors in references [21] and [22] propose adaptive inertia control strategies for ICs in ac/dc microgrid environments. Both proposed controllers modify the virtual inertia and capacitor parameter values to improve the transient response of interconnected grids, while the IC acts as a GF unit for the ac side. It is important to denote that these strategies do not aim

to equalise the interconnected grids. In reference [23], Watson and Lestas propose a controller for an ac/ac IC that combines the properties of dual-droop with matching control. The p.u. equalisation of frequencies is achieved, and the (unique) result shows that the transient response is improved as well since the intermediate dc bus inertia is used to stabilize ac systems. However, the main focus of the paper is on analysing the stability of interconnected grids through passivity, rather than assessing the control's performance in different scenarios and conditions.

In the last place, reference [24] proposes a *tie-line* method for an IC on a hybrid microgrid. Even if the control contributes to the p.u. equalisation of grids and power sharing, the inertial response coupling is not achieved. The proposed control compares ac frequency and dc voltage, and the difference is fed to a first-order filter to obtain the reference current for the IC's low-level control. This filter avoids sudden power transfer (and hence support), which does not replicate the inherent power transfer of a tie line has, as it is thoroughly described in Section 2.

All in all, even if most of the reviewed IC control techniques are able to equalise the interconnected systems in steady-state, and some others provide transient support to interconnected grids, none of the existing techniques replicate the behaviour of a power transmission line, extending its benefits beyond same nature interconnections. It is important to denote that these techniques do not offer GF capabilities (except for [21–23]), and they mainly appear focused on specific microgrid interconnections, lacking a generalised IC control approach to be employed at any type of link. With regard to the provided results, they are mainly focused on the power-sharing feature, and other aspects such as the coupling of inertia between the interconnected grids, the improvement of the transient or inertial response, the control performance under system failure, or grid scenarios beyond microgrid interconnections are not covered.

Here, a new control strategy for ICs named *virtual power line* (VPL) control is presented. This strategy emulates a purely inductive line by using the IC-based interconnection when grids of different natures, non-synchronised ac grids and grids of different voltage levels (either ac or dc) need to be connected. The VPL control not only contributes to the improvement of the steady-state responses of droop-governed grids but also the transient behaviour of interconnected grids, since it couples the inertial as well as the primary (droop) responses of both subgrids as they would be part of a unique power system. Here, two variants of the VPL control are presented. On the one hand, the *dual grid-supporting* VPL (DGS-VPL) technique is oriented to the interconnection of grids that are already in place, with the aim of supporting them as an equivalent power line would do. On the other hand, the *single grid-forming*-VPL (SGF-VPL) control offers the ability to form new power systems from existing ones while supporting both interconnected systems. This feature increases system reliability and helps in the investment reduction/deferral of new GF units. For example, when converter-interfaced RES generation units are installed in a remote area, the SGF-VPL strategy can be employed to form the grid by the IC, while RES units keep their focus on maximising the generated power instead of keeping the grid stable,

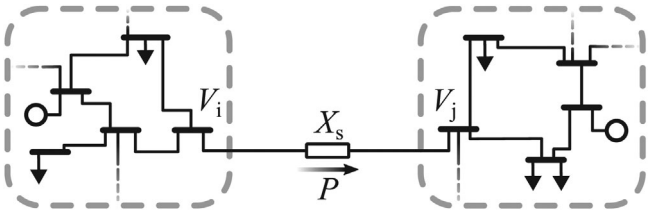

FIGURE 1 Two power systems tied by a power transmission line.

as it is further explained in Section 3.3. The VPL control does not require any communication or coordination with other grid agents for its operation, and its application range goes from high-power transmission-level links to microgrid links. However, it can be combined with higher-level coordinated controls or algorithms for system protection and black-start operation, as it is further specified in Section 4. Last but not least, it is important to denote that the application of VPL controllers to specific IC topologies has not been covered in the paper. The VPL has been considered as a part of the outer IC control loop, which needs to be accompanied by inner converter controllers, such as reference calculators, voltage or current inner loops. These loops will depend on the properties of interconnected grids, employed IC topology, number of power conversion stages and so on. In the presented study, the IC has been considered as a single controllable device able to exchange power among two subgrids, and even to form the grid at one of its sides. Therefore, the research has been focused on the demonstration of the properties and contributions of VPL controls, rather than evaluating it for specific IC topologies with specific inner control loops.

The upcoming sections are organised as follows: In Section 2, the bases of the proposed control are explained in detail. In Section 3, the effectiveness of the proposed VPL control is demonstrated in different grid scenarios by providing simulation results for each case. Section 4 provides practical implementation considerations, such as for the selection and tuning of the VPL control, or the possibility of combining it with higher-level algorithms. Finally, the paper is concluded with the most important remarks of the presented work in Section 5.

2 | VIRTUAL POWER LINE CONTROL

When transmission lines and transformers are employed for tying two power systems (Figure 1), the inertial (transient) and primary (steady-state) responses are coupled, meaning that all the devices participating in the grid regulation will respond under power perturbations, improving the frequency stability.

The proposed VPL control is inspired by the aforementioned inductive grid-tying devices, and therefore, the operation principle of an inductive transmission line for ac-ac and dc-dc connections is revised first. Then, based on the power transmission analogy through inductive elements on ac and dc systems, and taking this generalisation as a reference, the principles of the VPL control are presented. Taking advantage of the control flexibility offered by ICs, the inductive VPL concept is

extended to other connections beyond typical ac-ac and dc-dc system interconnections.

2.1 | Inductive power line tying two AC systems

If the power systems depicted in Figure 1 are ac, then the voltage at a node (V) represents the magnitude and angle of this voltage ($V\angle\theta$). If the two grids are interconnected at nodes i and j assuming a purely inductive line, the active power flowing through the line is obtained as follows:

$$P_{ac} = \frac{V_i V_j}{X_s} \sin \underbrace{\left(\theta_i - \theta_j\right)}_{\delta} \tag{1}$$

where X_s is the inductive impedance of the line, and V_i, V_j and θ_i and θ_j represent the voltage amplitudes and angles of the nodes i and j, respectively. If the angle difference δ remains small, Equation (1) can be simplified as:

$$P_{ac} \approx \frac{V_i V_j}{X_s} \underbrace{\left(\theta_i - \theta_j\right)}_{\delta} \tag{2}$$

Previous Equation (2) can be expressed in terms of frequency by applying the integral of the node angles:

$$P_{ac} \approx \frac{V_i V_j}{X_s} \underbrace{\int \left(\omega_i - \omega_j\right) dt}_{\delta} . \tag{3}$$

Assuming that the voltage amplitudes ($V_i V_j$) are relatively constant, and the inductive impedance (X_s) is constant as well, the active power transfer from one system to the other strongly depends on the angle difference δ at interconnection nodes i and j. It is important to remark that when two ac power systems are tied using an inductive line, the frequency of both grids is the same in steady-state due to the effect of droop-governed generators that form the grids. However, if the transient phenomena are observed, when sudden power variations occur, the frequencies of ac systems change and the power through transmission lines changes according to (3) until the frequencies become stable for the new operating point. Connecting ac power systems through transmission lines involves all the generators in the power response, increasing the system's robustness compared to the operation of decoupled grids.

2.2 | Inductive power line tying two DC systems

If the interconnected systems in Figure 1 are dc, the node voltages V_i and V_j correspond to dc voltage amplitudes. In such cases, the active power transfer from node i to node j depends on the integral of the voltage difference at their terminals, and the inductive value of the line (to simplify the analysis, the initial current through the line is not considered):

$$P_{dc} = \frac{V_i}{L_s} \int \left(V_i - V_j\right) dt. \tag{4}$$

Thus, when there is a voltage difference in the interconnected dc systems (i.e. at the terminals of the interconnection line), the active power will increase or decrease, and when V_i and V_j are equalised, the active power transfer will remain constant as described by (4). In other words, when power variations occur at droop-governed dc systems, the dc voltages at the terminals of the interconnection will be equalised once the generators stabilise at the new operating point, making the power through the dc line converge to a constant value. It is important to mention that in the same way, the power transmission through inductive ac lines causes a voltage drop, the line resistance causes a voltage drop in dc lines. However, even if ac and dc inductive transmission lines might have a resistive part, the transient behaviour for the active power (and hence the grid-coupling level) relies on the inductive part of the line. Therefore, the line resistance has not been considered in the aforementioned ac and dc line analyses, and it will neither be contemplated in the upcoming VPL control proposal.

2.3 | Virtual power line control for ICs

Sections 2.1 and 2.2 explain how the power transfer through ac and dc transmission lines is described by the equation of the inductance applied for each case. This section describes how the aforementioned principles are applied for the interconnection of any type of grid, regardless of its nature or voltage level, laying the foundations of the so-called VPL control.

From (3) and (4), it can be deduced that the active power transfer through an inductive line is directly related to the frequency in ac grids and to the voltage in dc ones. Based on this premise, an equivalence can be formulated to operate dc grids analogously to ac systems [25, 26]. When it comes to grid interconnection through ICs, the VPL control is a generalisation of this equivalence that enables to tie any type of grid (ac or dc, different frequency or voltage levels, etc.).

In order to achieve so, the first step is to convert ac frequencies and dc voltages to their corresponding per-unit values. These variables are henceforth referred as x_i and x_j, where x represents frequency in ac grids and voltage in dc ones. Assuming that voltage amplitudes are close to 1 p.u. either in ac or dc grids, the equation that describes the power transfer through a VPL interconnecting nodes i and j can be formulated as:

$$P^*_{VPL} = \frac{1}{Z_{VPL}} \underbrace{\int \left(x_i - x_j\right) dt}_{\delta_v} \tag{5}$$

where Z_{VPL} is the virtual inductive impedance parameter of the VPL control, and δ_v is the equivalent virtual angle difference between nodes.

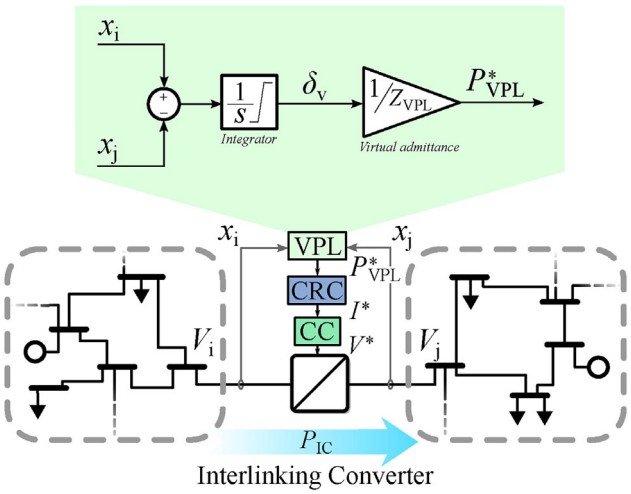

FIGURE 2 Representation example of an interlinking converter (IC) with the dual grid-supporting–virtual power line (DGS-VPL) control tying two power systems.

Even if the VPL control can be applied on an IC to interconnect systems of different natures, the synchronisation concept cannot be applied anymore. Instead, a *virtual synchronous reference frame* can be used, exchanging active power between incompatible grids according to this frame where the p.u. values of frequency (for ac grids) and voltage (for dc ones) are employed as inputs. Considering that x_i and x_j are the p.u. variables of the interconnected systems, they can be seen as *equivalent frequencies* to calculate the active power reference for the IC, employing the previously described Equation (5). It is important to denote that this frame is initialised when the VPL control starts its operation, so the flow of active power through the IC will act as *synchronising power*, driving the interconnected systems to a *virtual synchronisation*, achieving the same p.u. value at both sides of the IC. Hence, droop-controlled generators at both interconnected subgrids will face the same p.u. deviation and will provide active power proportionally according to it.

Based on (5), two different VPL control approaches are proposed subsequently, and their performance in different scenarios is comprehensively analysed in Section 3. It is important to remark that lower-level control loops are not considered in this study since they depend on aspects such as the IC topology or the nature of the interconnected systems, which are not covered in this study.

2.4 | DGS-VPL control

The DGS-VPL control loop and its conceptual implementation are depicted in Figure 2. This control directly implements (5) to obtain the power reference P^*_{VPL}. The p.u. values of interconnected nodes are subtracted and integrated, obtaining a *virtual angle* (δ_v) through the VPL. Then, applying the Z_{VPL} term, the active power reference is obtained. A current reference calculator (CRC) and an inner current controller (CC) are required to regulate the transferred power from one grid to the other [26]. Furthermore, these internal loops will protect the IC device and prevent it from over current conditions. It must be noted that internal control loops will depend on the nature of interconnected grids and the employed IC topology, so the DGS-VPL can be applied to carry out ac-ac, dc-dc or hybrid interconnections. The VPL controller contributes to unifying the p.u. values of grids at interconnection nodes, and this will be achieved unless the power limit of the IC is exceeded. In such cases, the integrator of the VPL control in Figure 2 will limit the active power reference P^*_{VPL} (and the CC will also limit the converter current as well). Then, if the p.u. measurements of interconnected systems become closer and drive the power reference below the saturation point, the VPL will retake its normal operation again.

Thus, the controlled variables (frequency in ac and voltage in dc systems) will converge to the same per-unit values as far as possible, as demonstrated in Section 3. Since the DGS-VPL provides a power reference, it can be easily implemented without modifying the inner control loops of the power converter. This is an advantage when the inner control is not accessible to the user, or when the converter manufacturer prefers not to modify that inner control structure.

In case one or both interconnected grids are ac, the voltage amplitude can be fixed to a certain value, or voltage and/or reactive power support control strategies similar to the ones studied in references [27–30] can be implemented in parallel to the VPL control, although they are not covered in this manuscript.

2.5 | SGF-VPL control

Generally, when power converters are employed as grid-forming units, they energise the grid from a voltage/power source (f.i., an ESS or a controlled dc bus). In the case of ICs, even if there is not a dedicated source, the reserve of one subgrid is employed to supply the subgrid at the other side of the IC. Thus, ICs can still be controlled as GF units at one of their sides (to set the frequency and/or voltage), if there is an existing grid at the other side [10]. With the SGF-VPL strategy, in addition to supporting the interconnected power systems as with the DGS-VPL, the IC is controlled as a GF device at one of its sides. This feature is essential when starting a new grid that needs to be energised at black-start operation. It must be considered that if a SGF-VPL IC is going to be connected to a grid which is already in place, a initial self-synchronisation stage is required before starting the VPL operation.

Depending on whether the formed grid is dc or ac, the implementation of the SGF-VPL is slightly different as explained hereafter. Although in the presented study inner voltage and current controllers are not studied, it must be noted that SGF-VPL requires these loops in order to set the grid voltage and safely operate the IC.

2.5.1 | DC SGF-VPL control

This VPL control variant is able to generate a dc grid at the terminals of the IC from a existing grid. If (5) is taken as reference,

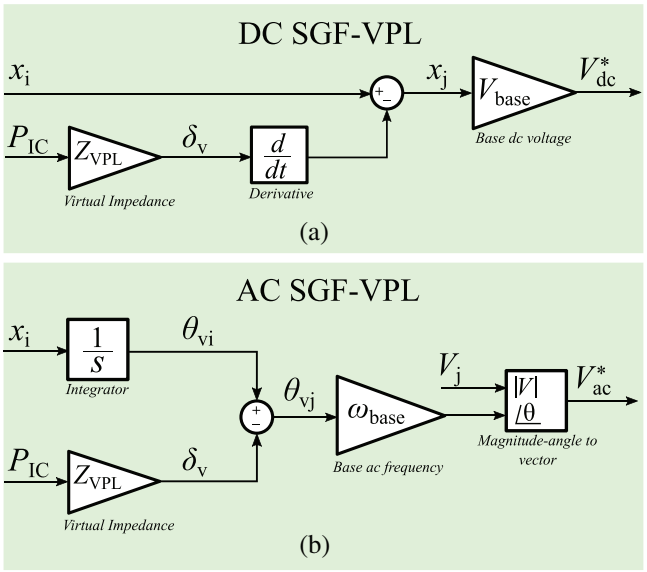

FIGURE 3 Detailed single grid-forming virtual power line (SGF-VPL) control scheme: (a) to form dc grids and (b) to form ac grids. IC, interlinking converter.

x_i corresponds to the p.u. value of the grid that is already set by other devices, and x_j corresponds to the p.u. value of the system created by the DC SGF-VPL control. Thus, if the value of x_j is isolated in (5), it is obtained that:

$$x_j \approx x_i - \frac{d}{dt}(P_{IC}Z_{VPL}) \tag{6}$$

It must be noted that the measured IC power (P_{IC}) is considered here as positive when the active power flows from node i to j.

The detailed control scheme that incorporates (6) to form dc systems from an existing grid (either ac or dc) is shown in Figure 3a. The voltage drop across the VPL impedance is calculated by deriving the measured IC power (P_{IC}) and the virtual impedance (Z_{VPL}) value. Then, this value is subtracted to the p.u. value of the existing grid (x_i) and the p.u. reference for the newly formed dc grid x_j is obtained. In the last place, the dc base value of the new grid is multiplied to obtain the dc voltage reference value, which will be fed to the inner IC voltage control loops.

With the DC SGF-VPL control, the obtained voltage response and IC power transfer will be the same as the one that is obtained when two grids are tied by a power line. When there is no power variation in any of the grids, the p.u. value of x_i will be equal to x_j. However, when there is a changing power flow through the IC, x_j will evolve according to the derivative of the virtual angle δ_v.

2.5.2 | AC SGF-VPL control

Since the SGF-VPL control is equivalent for creating ac and dc systems, the structure from Figure 3a can be employed to obtain the reference frequency for an ac system. In such cases, instead of using the base dc voltage, the base ac frequency should be employed in the last gain block. It is important to denote that for creating an ac grid, the IC will require the instantaneous reference angle position of the voltage vector, and thus, a continuous integrator must be added as well to the final stage in Figure 3a.

However, taking into consideration practical implementation aspects and with the aim of avoiding derivatives in control loops, Equation (5) has been reformulated as follows:

$$\int x_j\, dt = \int x_i\, dt - (P_{IC}Z_{VPL}). \tag{7}$$

In this case, x_j corresponds to the p.u. frequency of the newly formed ac system. The integral in the equation is kept because the GF control requires the instantaneous angle position of the ac voltage, which is obtained by integrating x_i and x_j. The virtual p.u. angles corresponding to these variables can be defined as follows:

$$\theta_{vi} = \int x_i\, dt$$

$$\theta_{vj} = \int x_j\, dt.$$

Hence, (7) can be reformulated as:

$$\theta_{vj} = \theta_{vi} - (P_{IC}Z_{VPL}). \tag{8}$$

Figure 3b shows the implementation of the AC SGF-VPL controller. To convert the p.u. to the absolute value of the angle, θ_{vj} is multiplied by the base frequency of the ac system.

The voltage amplitude and the reactive power control at the AC SGF-VPL approach can be defined by classical voltage or reactive power control schemes, and since it is considered that these strategies are already addressed in the literature, they are not contemplated in the actual study.

3 | PERFORMANCE OF THE VPL CONTROL

The aim of this section is to show the operation and assess the performance of the proposed VPL control variants under different power system scenarios. Taking into account that the VPL concept couples the interconnected grids, aspects like the transient and steady-state responses, or the amount of transferred active power for different VPL control parameters are studied hereafter.

The tests have been carried out using the *dynamic load flow–based* simulation tool proposed in reference [31, 34]. The employed tool is based on Matlab Simulink® software. It combines a reduced-order (electromechanical) generator and load models (implemented in Simulink), with a static load flow solver in Matlab that obtains node voltages and angles for given loading and generation conditions. In this tool, lower-level control loops are avoided, easily implementing different grid, generator,

TABLE 2 System and interlinking converter (IC) parameter values for the simplified hybrid simulation scenario. Abbreviation: VPL, virtual power line.

Device	Parameter	Value [p.u.]
AC grid G_1	H_1	3
	D_1	30
	τ_1	0.4
DC grid G_2	H_2	3
	D_2	30
	τ_2	0.4
IC - VPL	Z_{VPL}	0.01

load and IC control models with reduced computational burden and time cost (compared to EMT simulations). The purpose of the performed simulations is to assess the contribution to the frequency stability of the proposed controller by observing the rate of change of frequency or voltage (RoCoF and RoCoV), frequency nadir, damping and the operation point at steady-state after a disturbance, rather than looking at the electromagnetic phenomena occurring at the system. The specific simulation scenarios for testing the proposed VPL controls are explained in each case.

3.1 | Test I: DGS-VPL on a hybrid AC/DC grid link

In order to show the operation principle of the DGS-VPL control, a hybrid ac/dc simulation scenario has been employed where the ac grid corresponds to a 14-node IEEE system inspired by reference [32], and the dc one to a 9-node WSCC grid topology based on reference [33], as depicted in Figure 4. The power systems are tied through an IC, in which different control proposals are going to be deployed for testing in the upcoming sections. For the sake of simplicity, in this test, only one generator has been considered at each grid. In the ac grid, a simplified SG model has been employed, which includes the swing-equation, the governor with a classical primary regulator and the active voltage regulator as in reference [34]. In the dc grid, a virtual capacitor control has been implemented in the low-level control of a GF converter as explained in reference [26]. The primary regulator is equal for both generator models and comprises a droop control with a first-order low-pass filter. The aim of this test is not to represent in detail the interconnected grids and their generators, but rather to illustrate the principles of operation of the proposed DGS-VPL control from Figure 2.

The parameters of the generators of the interconnected grids are shown in Table 2. The most relevant parameters for this test are the inertia of generators (H), the droop gain of the primary regulators (D), the time constants of the primary regulators' delay (τ), and the VPL impedance Z_{VPL}.

Figure 5a shows the p.u. voltage and frequency at interconnection buses 6 and 12 from dc and ac grids, respectively, for a 0.5 p.u. active power load step applied at $t = 0.5$ s on the ac system, and at $t = 10.5$ s on the dc system (see Figure 5c). Thanks to the interconnection through the DGS-VPL-controlled IC, the frequency and voltage of the interconnected grids converge to the same value in steady-state. Besides, if the decoupled grid scenario is taken as a reference (with its nadir and RoCoF/V values), the frequency nadir and RoCoF for the ac grid are improved by 28.36% and 22%, respectively, while for the dc case, the voltage nadir and RoCoV are reduced by 32.74% and 47%. Figure 5b shows how the virtual delta angle δ_v varies its value when active power load steps are applied in both systems, causing an active power transfer between the interconnected grids, proportional to the inverse of the Z_{VPL} value.

With the aim of studying more in-depth the effect of the value of Z_{VPL} in the response of the interconnected systems, Figure 5d,e depicts the frequency and voltage responses of the generators from ac and dc systems for the previously stated loading conditions but for Z_{VPL} values ranging from 0.1 and decreasing it to 0.002. It is important to denote that the IC power ratio has been considered to be 0.3 p.u. (using the same base power as for ac and dc grids from Figure 4), limiting its maximum power contribution in both senses to such value. Therefore, Z_{VPL} parameters have been selected considering the power limitation (Figure 5f), and taking into account the aspects presented in Section 4.2. The results show how, the lower the value of Z_{VPL} is, the more coupled the interconnected systems are. This phenomenon is reflected in Figure 5f, where the IC power transfer dynamics increase for lower Z_{VPL} parameter values, improving the response of interconnected grids in Figure 5d,e. To be more precise, if the p.u. values of ac and dc grids for the $Z_{VPL} = 0.1$ are taken as reference, the frequency nadir and RoCoF values are decreased by 25.58% and 22.8% when Z_{VPL} is 0.002 (Figure 5d at $t = 1$ s). Similarly, voltage nadir and RoCoV values for the dc grid are reduced by 36% and 49.6% when the grids are strongly tied (Figure 5e at $t = 11$ s). Besides, it can be observed that for smaller Z_{VPL} values in Figure 5d,e, the settling time is reduced by 40%, with a reduced number of oscillations and higher damping. When higher Z_{VPL} values are employed at the VPL control, although the power system that has suffered the load variation presents a higher RoCoF/V and nadir, the contrary grid does not suffer the variation in the same level (lower coupling).

In short, when the DGS-VPL control is deployed on an IC, the inertial response and the prime movers' response of the interconnected systems are coupled, making all the devices participate in the regulation of the system and converge to the same steady-state value. Lower Z_{VPL} values will entail a stronger grid coupling and hence a better transient support under load variations.

3.2 | Test II: DGS-VPL versus existing IC control strategies

The aim of this section is to compare the proposed DGS-VPL technique with already proposed IC control approaches. For that purpose, a combination of IC control strategies that offer similar features have been employed. One of the most

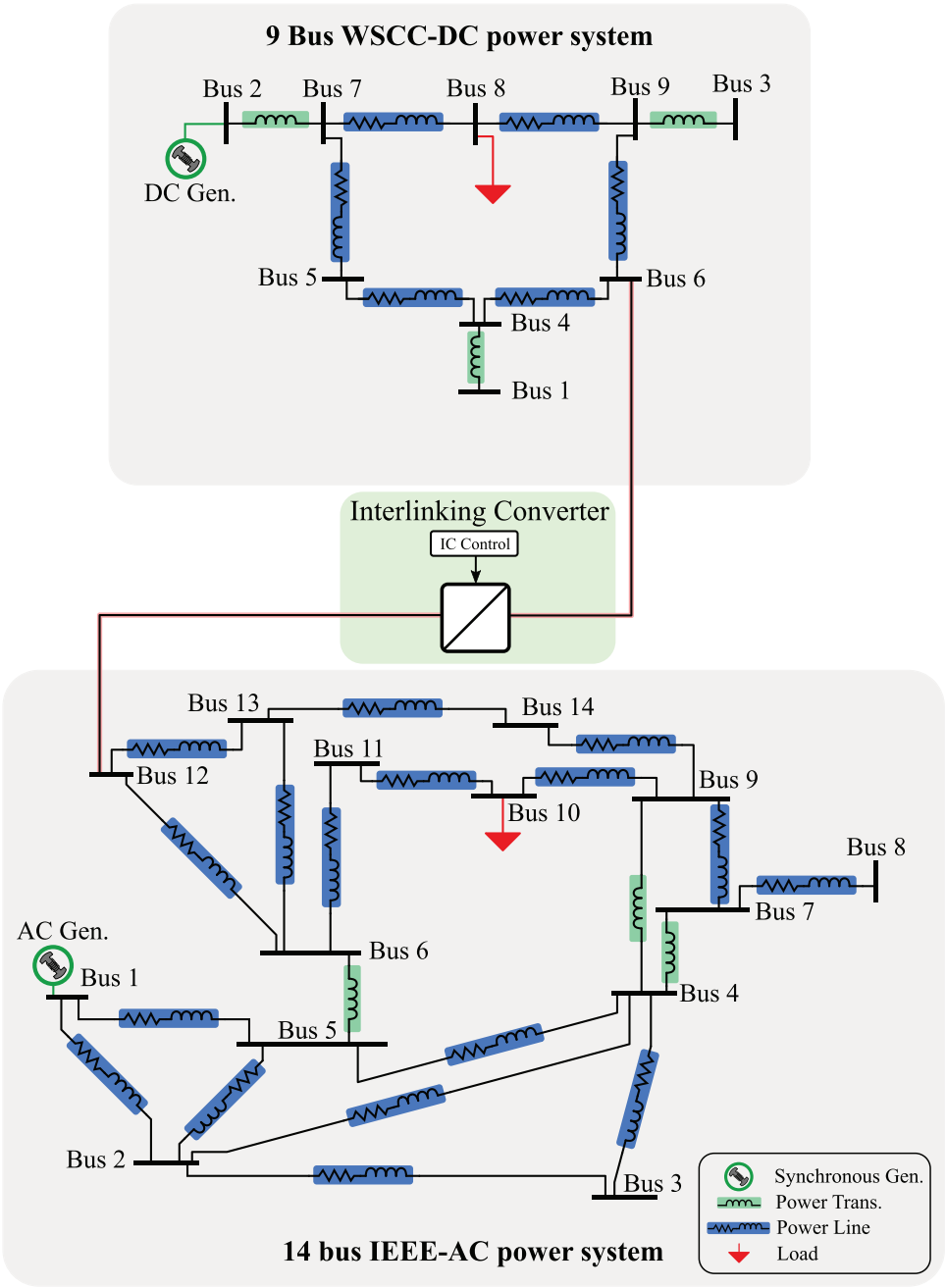

FIGURE 4 9-node WSCC system topology [33] with a dc generator and 14-node IEEE ac grid [32] tied through an IC.

common IC control strategies that contributes to unifying the primary response of interconnected grids is the so-called dual-droop (DD) control [10]. This DD control can be combined with the so-called dual inertia-emulation (DIE) [35], or other similar techniques like the ones proposed in references [36, 37] (which are able to provide virtual inertia to both interconnected grids) so that the IC also participates in the regulation of the transient response of the interconnected grids. In the following tests, the DIE-DD technique is employed as the benchmark for the comparison with the proposed DGS-VPL control.

The test scenario is the same as in the previous section (see Figure 4), and the parameters employed in the simulation are gathered in Table 3.

The results of the test are shown in Figure 6 (for the same load profiles as in the previous case, refer to Figure 5c). Figure 6a shows that the ac frequency and dc voltage (x_1 and x_2) converge to the same point almost instantaneously due to the strong coupling that the DGS-VPL offers (low Z_{VPL} value). In other words, the transient response benefits from the support of all the devices participating in the regulation of the grid. In the case of the DIE-DD control, the point of operation of

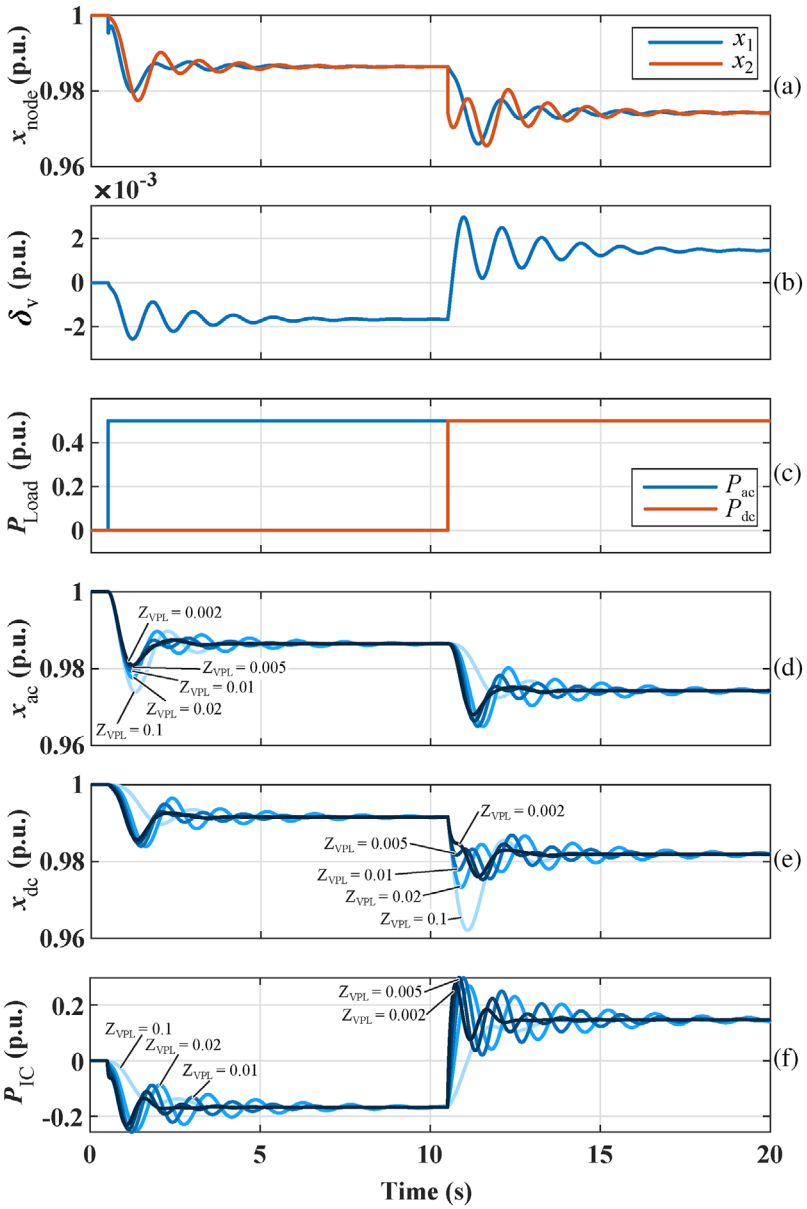

FIGURE 5 Virtual power line (VPL) operation concept test: (a) frequency of ac system (x_1) and voltage of dc system (x_2) (both in p.u.) at interconnection nodes, (b) virtual angle δ_v, (c) active power profiles at ac and dc systems, (d) frequency of the unique generator at the ac grid for different Z_{VPL} values, (e) voltage of the unique generator at the dc grid for different Z_{VPL} values, and (f) interlinking converter (IC) active power transfer for different Z_{VPL} parameter values.

TABLE 3 System and interlinking converter (IC) parameter values for IC control comparison. Abbreviations: DIE, dual inertia-emulation; DD, dual-droop; VPL, virtual power line.

Device	Variable	Value [p.u.]
IC - DIE	H_{V_1}	2
	H_{V_2}	2
IC - DD	D_{d_1}	10
	D_{d_2}	10
IC - VPL	Z_{VPL}	0.002

each grid in the steady state depends on the D_d droop parameters, and the transient response of each grid is affected by the virtual inertia parameters (H_V) at the DIE algorithm [35].

Figure 6b illustrates the active power through the IC, where the power response in the DGS-VPL control is 1.88 times higher in amplitude, both during transients and in steady state. The steady-state value of the DGS-VPL power reference depends only on the droop controllers from ac and dc grids, while the transient response is in accordance with the stronger coupling of grids (Z_{VPL} parameter) and their inertias as has been shown in the previous test.

3.3 | Test III: SGF-VPL control operation

In the previous tests, the grid-supporting VPL variant has been compared with a DD-DIE technique, and it has been observed that these controllers react under frequency and voltage perturbations but are not capable of forming a grid by themselves as explained in Section 2.5. However, modern converter-dominated power system scenarios require a minimum amount of grid-forming devices to set the system voltage and frequency and ensure a stable operation. Considering the

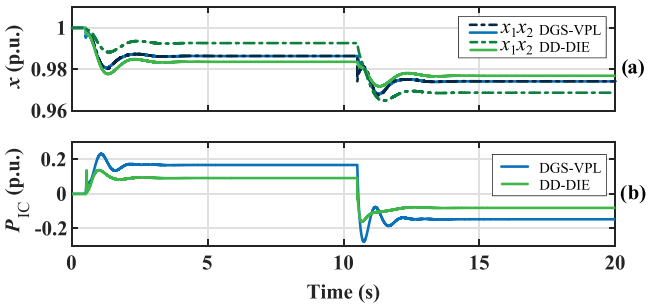

FIGURE 6 Virtual power line (VPL) operation compared to dual inertia-emulation dual-droop (DIE-DD) interlinking converter (IC) control: (a) frequency (x_1) and voltage (x_2) of ac and dc systems for both IC control approaches and (b) active power transfer for each control strategy.

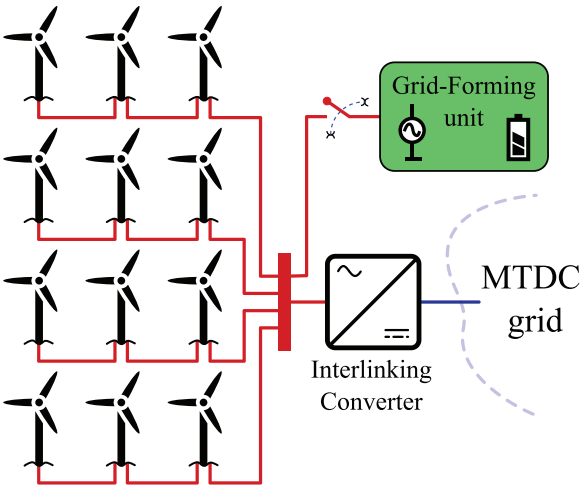

FIGURE 7 AC wind power plant topology example with ac/dc interlinking converter (IC) link.

offshore ac power system from Figure 7, which transmits the generated power through a dc link, the WP park will require at least one GF unit for its adequate operation. Thus, at least one of the WP generators, the IC or an external ESS must operate as the grid-forming unit to set the system's ac voltage and frequency. It is important to denote that even if some WP generator technologies can contribute to forming the grid, the regulation capacity under grid events is limited by the energy stored at dc bus capacitor of power converters, as Li et al. explain in reference [38]. Even if these solutions can contribute to making the system more reliable, the regulation capacity that a SGF-VPL-controlled IC can provide is much higher. This happens due to the fact that the voltage is formed by taking as the energy source the contrary grid, which might present a much higher capacity than the dc bus capacitor of a wind turbine. Besides, it is very important to denote that, unlike converter-based RES units, the SGF-VPL control can energise a power system at black-start operation from the contrary grid, as it is further explained in Section 4.3. Therefore, the implementation of a SGF-VPL control is very interesting for setting the reference of the WP grid, and it can coexist with other grid-forming devices like the one proposed in reference [38].

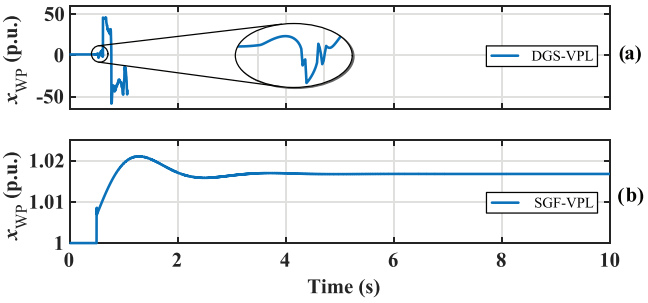

FIGURE 8 Disconnection of the main grid-forming (GF) unit from the WP plant with (a) dual grid-supporting virtual power line (DGS-VPL) control and (b) single grid-forming VPL (SGF-VPL) control.

In the test scenario from Figure 7, a converter-interfaced ESS has been set as the main GF unit of the WP grid, so that this test aims to show the advantages of the SGF-VPL control over other dual grid-supporting control techniques when the main GF unit fails. The disconnection of this device has been simulated in two cases: with the IC controlled as a DGS-VPL, and as a SGF-VPL. The employed Z_{VPL} parameter for both tests is the same ($Z_{VPL} = 0.01$).

Previous to the failure of the main GF unit, the power system operates in stable voltage and frequency conditions, and the GF ESS is being charged by the power generated by the WP turbines. Figure 8a shows that when the GF unit fails—that is, suddenly disconnects—at $t = 0.5$ s, the DGS-VPL control of the IC is not able to maintain the frequency of the WP system, leading to a system instability caused by the lack of other GF unit in the system. On the contrary, if the SGF-VPL control is deployed at the IC, Figure 8b shows how for the same test conditions the power system does not become unstable. In this case, the IC is able to set the system's frequency and transfer the power generated by the WP generators to the MTDC grid when the GF unit fails. This power transfer to the dc grid entails an increment of 1.7% in the frequency and voltage of the droop-governed ac/dc system.

These results demonstrate that the proposed SGF-VPL control is useful in improving the reliability of converter-dominated power systems, since the IC is able to operate as a GF unit at one of its sides. This will help to reduce the number of GF units required in the grid, and can be useful to avoid new infrastructure investments, for example, for the installation of ESSs. Besides, this control decreases the chances of a possible blackout if the rest of the GF units connected to the system fail.

3.4 | Test IV: SGF-VPL ICs forming AC and DC grids in a multi-grid system

This test shows that in addition to the GF capability, the properties of the SGF-VPL control are of high interest for the interconnection of various power systems or different parts of a grid. For that purpose, the multi-grid power system scenario from Figure 9 has been set up, where four ac power systems are tied through an MTDC grid. The main two ac

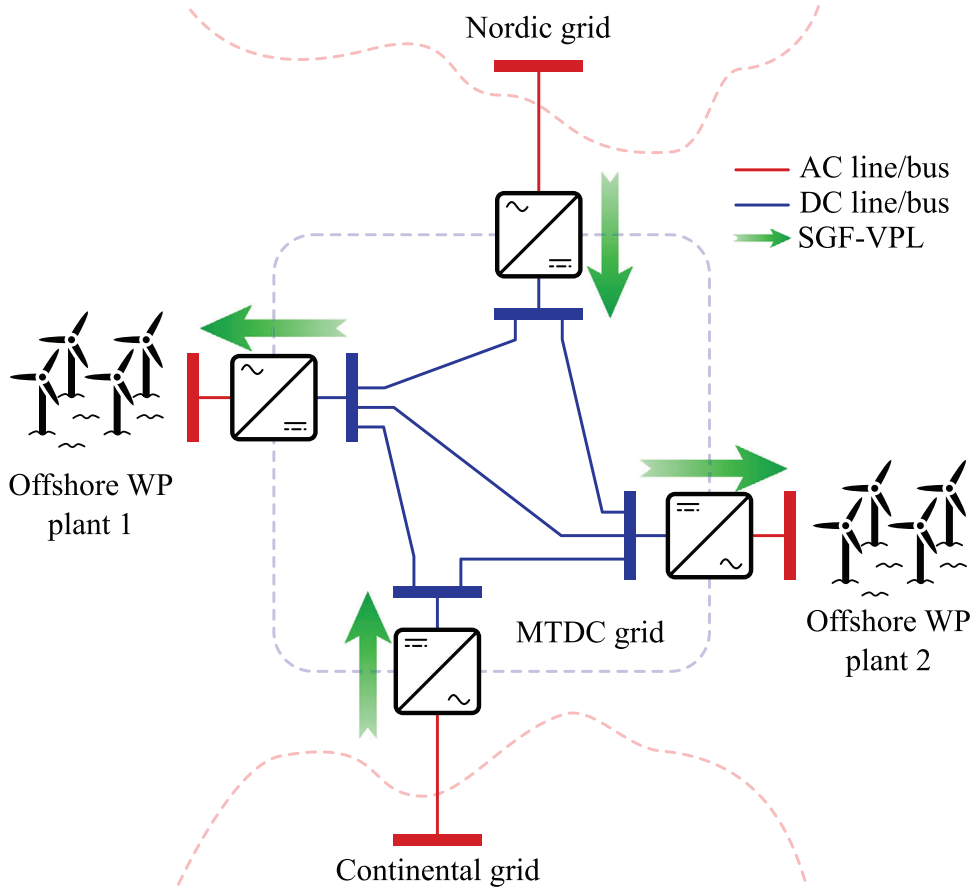

FIGURE 9 Simplified diagram of the hybrid ac/dc benchmark scenario with representation of grid-forming (GF) interlinking converters (ICs) implementing the single grid-forming virtual power line (SGF-VPL).

power systems correspond to a 32-bus Nordic grid proposed by CIGRÉ Task Force 32.02.08 in reference [39], and a Continental European HV transmission network proposed by the CIGRÉ Task Force C6.04.02 in reference [40]. Each grid model includes a synchronous generator-based power generation unit to represent the aggregated dynamic response of the grid as in Test III. Besides, two WP ac grids are included, which consist of simplified 5 bus systems as represented in Figure 7. In this case, the SGF-VPL–controlled ICs are responsible for forming the WP ac grids as shown in Figure 9. Similarly, the MTDC grid is formed by the ICs interfacing the Nordic and Continental grids by employing the dc variant of the SGF-VPL control. The employed Z_{VPL} parameter is equal for all the SGF-VPL–controlled ICs, with a value of $Z_{\mathrm{VPL}} = 0.01$.

Figure 10a–d shows the evolution of all the subgrids when the aggregated WP generation and load profiles (represented in Figure 10e,f) are applied to the different power systems. With the aim of coupling all the grids, the ICs are controlled with their corresponding SGF-VPL technique as illustrated in Figure 9. This coupling can be corroborated by looking at the grids' frequencies and voltages. Some differences can be appreciated in the p.u. values of the different grids, caused by the voltage drops in the MTDC system lines (which correspond to the resistive part of the transmission lines). However, all of the waveforms present a very similar dynamic behaviour due to the coupling provided by the ICs. By looking at Figure 10c,d, it can be seen how the Nordic system is more susceptible to load variations compared to the Continental system. This happens because the total inertia connected to the Nordic grid is 10 times lower than that of the Continental grid (find the system parameters employed in reference [31]).

Figure 11 represents the active power transferred by the SGF-VPL–controlled ICs in the previous scenario. The ICs that set the voltage and frequency in the WP systems transfer all the active power generation to the MTDC grid, which is reflected as a negative power according to (8) and shown in Figure 11a. The ICs that link the Continental and Nordic grids with the MTDC and are in charge of forming the MTDC system and support the Continental and Nordic grids by supplying active power under sudden load perturbations, which are reflected as negative power values according to (6) in Figure 11b,c.

The obtained results demonstrate how the VPL control supports the interconnected systems during transients as well as steady-state operation analogously to a classical transmission line. Therefore, when subgrids are connected using VPL-controlled ICs, they can be considered an extension of the same grid. In this sense, active power flow through subgrids of different natures will naturally occur from areas with generation

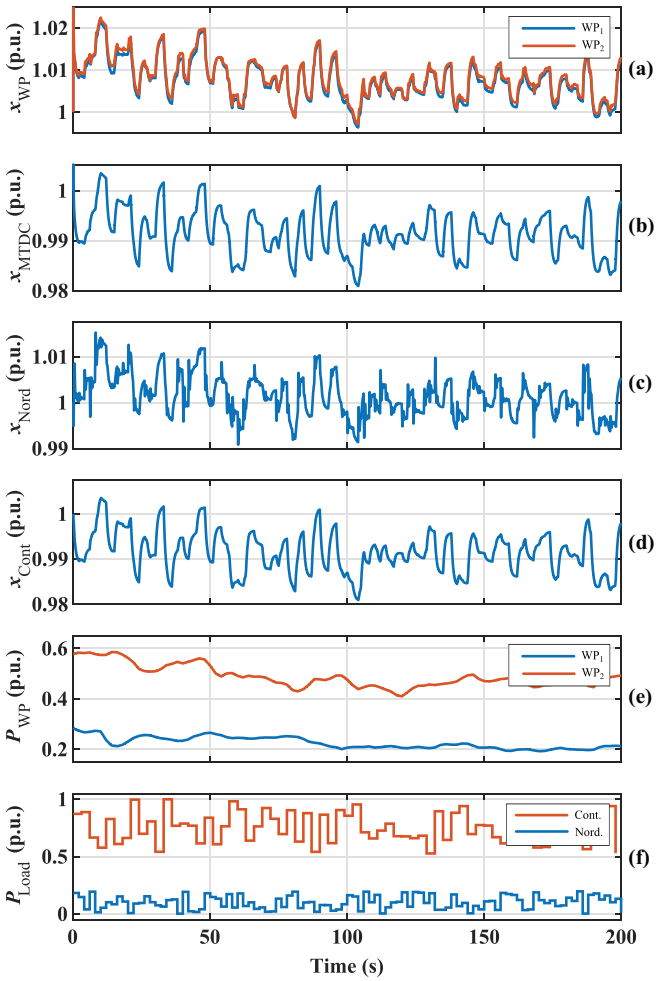

FIGURE 10 (a) Frequency of the wind power (WP) ac systems, (b) voltage of the MTDC grid, (c) frequency of the Nordic grid, (d) frequency of the Continental grid, (e) aggregated active power generation of the WP plants and (f) aggregated active power loading of Nordic and Continental systems.

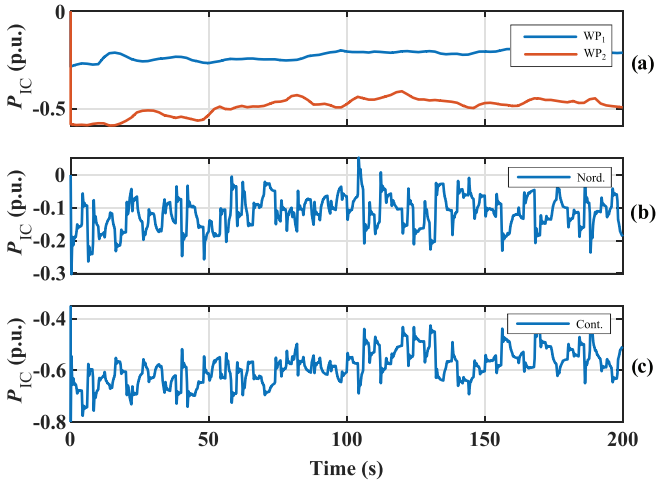

FIGURE 11 Single grid-forming virtual power line (SGF-VPL) controlled interlinking converter (IC) power of (a) WP-MTDC links, (b) Nordic-MTDC link and (c) Continental-MTDC link. WP, wind power.

to areas with more demand, without the need for any communication or coordination among the different ICs. Unlike other GF techniques proposed in the literature, the SGF-VPL control is capable of supporting both sides of the IC under power perturbations. This improves the coupling between different grids or parts of the grid, which is especially relevant for systems decoupled from strong grids or systems dominated by electronic converters. Apart from the scenarios already described in the paper, the SGF-VPL control can be a feasible solution for ICs operating at high voltage dc (HVDC) links tying ac systems, improving the transient and steady-state coupling of the interconnected ac and dc buses.

It is important to highlight that the VPL control is compatible with any upper-level secondary controller since it employs local measurements to carry out the IC control.

4 | PRACTICAL IMPLEMENTATION CONSIDERATIONS

The VPL control offers a flexible strategy for ICs to connect electrical grids under diverse scenarios. However, its practical application requires a careful balance between stability and performance. This section addresses the key factors for Z_{VPL} tuning and control mode selection, emphasizing the necessity of considering stability analyses for proper configuration. It is essential to highlight that the optimal settings for Z_{VPL} and the VPL operation depend heavily on the specific characteristics of the interconnected grids, as actions suitable for one scenario may be detrimental in another.

4.1 | Grid-forming and grid-supporting VPL operation

Even if DGS-VPL and SGF-VPL techniques reside on the same principles, the impact on the stability of interconnected grids might be very different depending on the employed VPL control philosophy.

As authors state in references [41, 42], grid-supporting controllers present a delay in the power reference calculation and setting. In the case of the DGS-VPL control, if this is combined with a too-small Z_{VPL} value, small perturbations can lead to a big transferred power by the IC, affecting negatively interconnected grids. Thus, transient instability is more likely to occur in converters that are connected to weak grids, or those which are injecting higher power [43].

Consider the case where the DGS-VPL IC links a strong grid with a microgrid. If a sudden load variation occurs at the microgrid, a small Z_{VPL} value (strong coupling) will lead to an excessively big power transfer at the IC, making the small system's inertia accelerate or even lose synchronism. In such a scenario, authors recommend employing a relatively big Z_{VPL} value (weaker coupling) that will assure stability and steady-state power dispatch. However, if the interconnected grids have similar properties as in Test I (Section 3.1), Z_{VPL} can have smaller

values at the DGS-VPL, transferring more power and having a stronger coupling of the grids.

In contrast, if the IC is operating as a SGF-VPL for the microgrid, the IC will hold the smallest grid, improving substantially its frequency stability. The loading of the smallest grid will have a damping effect on the biggest grid's inertia, improving the overall stability [42]. So in this case, a smaller Z_{VPL} value can be employed to make the coupling stronger, improving stability.

4.2 | VPL parameter selection

When choosing the Z_{VPL} parameter, authors recommend considering the following aspects at the interconnected grid scenario:

Active power transfer limitation at the IC

The active power transfer needs to be limited by inner control loops in order to protect the IC. If the p.u. deviations at interconnected grids are so large, or they persist for too long, the power saturation limit of the IC will be achieved. In the following, the effect of the IC power and the VPL parameter is analysed for steady-state and transient responses.

Contribution of the IC power to the total loading of grids and the droop-based generators (steady-state)

The p.u. equalisation of interconnected grids will only be achievable if the synchronising VPL power is below the saturation point. In such case, the VPL will drive droop generators from both grids to same p.u. frequency and voltage values (except from the resistive deviations at dc lines). In case the IC power limit is achieved, the droop-governed generators from both grids will converge to different values. Therefore, the Z_{VPL} parameter will have no effect at steady-state in the primary response, and the convergence to the same p.u. value will be limited by the capabilities of the IC.

Contribution of the IC power to the inertial response of grids (transient)

The transient response of each grid mainly depends on the amount of inertia, the equivalent droop, the delay of primary movers and the magnitude of the power variations. Therefore, the authors recommend adjusting the Z_{VPL} parameter so that the maximum IC transient power is achieved when the worst permissible RoCoF/V and nadir situations occur.

All in all, the optimum Z_{VPL} parameter value will depend on the properties of the interconnected grids and the specific requirements for the VPL-controlled IC to keep the grids within safety boundaries.

4.3 | Operation mode selection and coordination of VPL-controlled ICs

Throughout the paper, it has been demonstrated that the VPL controllers operate effectively using local measurements, without any communication link or coordination. However, the authors foresee that the contributions of the proposed VPL controllers can be maximised by making them operate in a coordinated way or using higher-level algorithms.

In previous sections, it has been demonstrated how the Z_{VPL} parameter does have an impact on the transient response of grids, but it does not at the steady-state power dispatch. Therefore, Z_{VPL} could be increased (weak coupling) when the interconnected grids' situation is good and reduced (strong coupling) when more coupling and transient support are required.

Beyond static tuning, dynamically adjusting Z_{VPL} in real-time offers further potential for improving stability and damping of sub-synchronous inter-area power oscillations through the IC, employing similar approaches to the ones that authors propose in references [44–46].

Besides, the operation mode of the IC can be modified by changing the SGF-VPL mode from one grid to the other. This concept is presented in reference [23], named as 'partially grid-forming', and suggested for use to support the weakest grid while the other side of the IC works as a grid-following (in this case, as a grid-supporting VPL). This concept can be extended to enable the black-start operation of grids after a blackout. For instance, if a strong grid is connected to a microgrid through an IC, during normal operation, the IC can act as an SGF-VPL mainly supporting the microgrid. However, if the IC detects a cascading outage or failure at the strong grid (leading the strong system to a blackout), it can be used to isolate and protect the microgrid from the outage. Then, the IC can be ordered to operate as SGF-VPL to black-start the affected grid. In this case, the reserve from the microgrid will be used to energise the affected grid, enabling it to gradually connect all the generators and loads again. In such a way, ICs with coordinated-and-local protection algorithms and SGF-VPL controllers can be employed for system-wide restoration on a grid-of-grids scenario, reducing the outage time and affected user areas.

5 | CONCLUSION

This paper presents a VPL control concept for interlinking converters, which enables tying of different and incompatible electric systems—that is, ac-ac links with different frequencies and voltages, hybrid links, and dc-dc links with different voltage levels—analogously to an inductive transmission line interconnecting two compatible grids. The VPL control can be deployed at grid links of different scales, and it makes it possible to couple the transient and steady-state responses of the interconnected grids by employing only local measurements, improving the system's overall reliability.

Two VPL control variants have been proposed: the DGS-VPL and the SGF-VPL control. Although both techniques employ the same control principle—imitating the behaviour of a traditional inductive transmission line—the former equalises the interconnected grids only by transferring active power among grids, while the latter extends the VPL concept to offer grid-forming capabilities at one of the sides of the IC. This makes it possible to set the voltage and frequency of the system without the need for any other GF device and enables the formation of remotely located grids by the IC, reducing or avoiding

investments in installing additional devices such as ESS-based GF units or modifying the existing RES generation units.

The results have demonstrated how both VPL control variants contribute to equalise the voltages and frequencies of the interconnected systems, by coupling them in terms of inertia and primary response. Specifically, the implementation of the VPL control has improved the frequency and voltage nadir values of ac and dc grids by 36%, while the RoCoF and RoCoV have been decreased by 49.6%, with a 40% faster convergence time to steady-state values after a power disturbance. Moreover, it has been observed that the flow of active power occurs naturally from generation to consumption nodes as if all devices were part of the same electric system.

AUTHOR CONTRIBUTIONS

Julen Paniagua is responsible for the development of the idea, particularly the grid-forming approach; contributed to the writing of the paper; set up the simulation scenarios; obtained and processed the results; and developed most of the figures. Eneko Unamuno contributed to the development of the idea, writing, revising, and improving the content of the paper; interpreted the results; conducted a part of the state of the art revision; defined the simulation scenario; and developed the testing scenario figures. Jon Andoni Barrena proposed the original concept, planting the seed for the idea of the control strategy and contributed by revising the text and structuring the paper.

ACKNOWLEDGEMENTS

This work has been partially funded by the Basque Government under the project EP4H2 (KK-2022/00039) and RESINET (KK-2023/00042).

CONFLICT OF INTEREST STATEMENT

The authors declare no conflicts of interest.

DATA AVAILABILITY STATEMENT

The data that support the findings of this study are available from the corresponding author upon reasonable request.

ORCID

Julen Paniagua https://orcid.org/0000-0002-9984-8495
Eneko Unamuno https://orcid.org/0000-0002-2819-9635
Jon Andoni Barrena https://orcid.org/0000-0002-2237-4869

REFERENCES

1. Holttinen, H., et al.: System impact studies for near 100% renewable energy systems dominated by inverter based variable generation. IEEE Trans. Power Syst. 37(4), 3249–3258 (2022)
2. Hatziargyriou, N., et al.: Definition and classification of power system stability—revisited & extended. IEEE Trans. Power Syst. 36(4), 3271–3281 (2021)
3. Milano, F., et al.: Foundations and challenges of low-inertia systems (Invited Paper). In: 2018 Power Systems Computation Conference (PSCC), pp. 1–25. IEEE, Piscataway, NJ (2018)
4. Tielens, P., Van Hertem, D.,: The relevance of inertia in power systems. Renewable Sustainable Energy Rev. 55, 999–1009 (2016)
5. Mousavi, M.H., CheshmehBeigi, H.M., Ahmadi, M.,: A DDSRF-based VSG control scheme in islanded microgrid under unbalanced load conditions. Electr. Eng. 105(6), 4321–4337 (2023)
6. Starke, M., Tolbert, L.M., Ozpineci, B.: AC vs. DC distribution: A loss comparison. In: 2008 IEEE/PES Transmission and Distribution Conference and Exposition, vol. 22, no. 4, pp. 1–7. IEEE, Piscataway, NJ (2008)
7. Jovcic, D., Ooi, B.T.,: Developing DC transmission networks using DC transformers. IEEE Trans. Power Delivery 25(4), 2535–2543 (2010)
8. Justo, J.J., Mwasilu, F., Lee, J., Jung, J.W.: AC-microgrids versus DC-microgrids with distributed energy resources: a review. Renew. Sustain. Energy Rev. 24, 387–405 (2013)
9. Najafzadeh, M., et al.: Recent contributions, future prospects and limitations of interlinking converter control in hybrid AC/DC microgrids. IEEE Access 9, 7960–7984 (2021)
10. Ordono, A., Unamuno, E., Barrena, J.A., Paniagua, J.,: Interlinking converters and their contribution to primary regulation: a review. Int. J. Electr. Power Energy Syst. 111, 44–57 (2019)
11. Loh, P.C., Li, D., Chai, Y.K., Blaabjerg, F.,: Autonomous control of interlinking converter with energy storage in hybrid AC-DC microgrid. IEEE Trans. Ind. Appl. 49(3), 1374–1382 (2013)
12. Morais, A.S., Lopes, L.A.: Interlink converters in DC nanogrids and its effect in power sharing using distributed control. In: 2016 IEEE 7th International Symposium on Power Electronics for Distributed Generation Systems (PEDG), pp. 1–7. IEEE, Piscataway, NJ (2016)
13. Yoo, H.J., Nguyen, T.T., Kim, H.M.,: Multi-frequency control in a standalone multi-microgrid system using a back-to-back converter. Energies 10(6), 822 (2017)
14. Aggarwal, A., Siddiqui, A.S., Mishra, S.: Proportional load sharing in an autonomous hybrid micro-grid using interlinking converter. In: 2022 IEEE International Conference on Power Electronics, Smart Grid, and Renewable Energy (PESGRE), pp. 1–5. IEEE, Piscataway, NJ (2022)
15. Jianfang, X., et al.: Energy management system for control of hybrid AC/DC microgrids. In: 2015 IEEE 10th Conference on Industrial Electronics and Applications (ICIEA), pp. 778–783. IEEE, Piscataway, NJ (2015)
16. Shi, H., Sun, K., Li, Y., Wu, H.: Virtual transformer control for DC-DC interlinking converters in DC microgrids. In: 2019 IEEE Energy Conversion Congress and Exposition, ECCE 2019, vol. 1, pp. 4268–4273. IEEE, Piscataway, NJ (2019)
17. Baharizadeh, M., Karshenas, H.R., Guerrero, J.M.,: An improved power control strategy for hybrid AC-DC microgrids. Int. J. Electr. Power Energy Syst. 95, 364–373 (2018)
18. Mortezapour, V., Lesani, H.,: Hybrid AC/DC microgrids: A generalized approach for autonomous droop-based primary control in islanded operations. Int. J. Electr. Power Energy Syst. 93, 109–118 (2017)
19. Golsorkhi, M.S., Savaghebi, M.,: A decentralized control strategy based on V-I droop for enhancing dynamics of autonomous hybrid AC/DC microgrids. IEEE Trans. Power Electron. 36(8), 9430–9440 (2021)
20. Wang, J., Huang, W., Tai, N., Yu, M., Li, R., Zhang, Y.: A bidirectional virtual inertia control strategy for the interconnected converter of standalone AC/DC hybrid microgrids. IEEE Trans. Power Syst. 39(1), 745–754 (2024)
21. Zhang, L., et al.: An adaptative control strategy for interfacing converter of hybrid microgrid based on improved virtual synchronous generator. IET Renewable Power Gener. 16(2), 261–273 (2022)
22. Wang, J., et al.: A bidirectional virtual inertia control strategy for the interconnected converter of standalone ac/dc hybrid microgrids. IEEE Trans. Power Syst. 39(1), 745–754 (2024)
23. Watson, J.D., Lestas, I.,: Control of AC-AC interlinking converters for multi-grids. IEEE Trans. Smart Grid 15(4), 3390–3401 (2024)
24. Agrawal, S., Tyagi, B., Kumar, V., Sharma, P.: Interlinking converter operation in hybrid microgrid as a tie-line. In: 2022 IEEE International Conference on Power Electronics, Drives and Energy Systems (PEDES), pp. 1–6. IEEE, Piscataway, NJ (2022)
25. Unamuno, E.: Control and stability of AC/DC microgrids. PhD Thesis, Mondragon Unibertsitatea—Goi Eskola Politeknikoa (2017)
26. Unamuno, E., Paniagua, J., Barrena, J.A.,: Unified virtual inertia for ac and dc microgrids: and the role of interlinking converters. IEEE Electrif. Mag. 7(4), 56–68 (2019)
27. Nutkani, I.U., et al.: Intertied ac-ac microgrids with autonomous power import and export. Int. J. Electr. Power Energy Syst. 65, 385–393 (2015)

28. Lee, Y.D., Park, S.Y.: Reactive power support capabilities of nonsynchronous interconnection systems in microgrid applications. In: Conference Proceedings - IEEE Applied Power Electronics Conference and Exposition—APEC, pp. 125–131. IEEE, Piscataway, NJ (2016)
29. Hunziker, C., Schulz, N.,: Potential of solid-state transformers for grid optimization in existing low-voltage grid environments. Electr. Power Syst. Res. 146, 124–131 (2017)
30. Liu, Y., et al.: A coordinated control for photovoltaic generators and energy storages in low-voltage AC/DC hybrid microgrids under islanded mode. Energies 9(8), 651 (2016)
31. Paniagua, J., et al.: A dynamic frequency-and-voltage power flow simulation tool for hybrid AC/DC power systems based on Simulink. In: IECON 2022-48th Annual Conference of the IEEE Industrial Electronics Society, pp. 1–6. IEEE, Piscataway, NJ (2022)
32. Vijay Vittal, A.A.F., McCalley, J.D., Anderson, P.M.: Power System Control and Stability. 3rd ed. Wiley, New Delhi, India (2002)
33. Dembart, B., et al.: Power system dynamic analysis: Phase I. Final report. Technical Information Center. U.S. Department of Energy (1977)
34. Paniagua, J., Unamuno, E., Barrena, J.A., Serrano-Jiménez, D., Goikoetxea, A. Dynamic frequency-and-voltage power flow-based simulations of AC, DC and hybrid AC/DC power systems. In: Frequency and ROCOF measurement techniques and their applications for power systems, 1st ed., Shahnia, F., Liu, Y., Attilio Pegoraro, P. (Eds). Murdoch, Australia: Springer, 2025
35. Paniagua, J., Unamuno, E., Barrena, J.A.,: Dual inertia-emulation control for interlinking converters in grid-tying applications. IEEE Trans. Smart Grid 12(5), 3868–3876 (2021)
36. Rakhshani, E., Remon, D., Mir Cantarellas, A., Rodriguez, P.,: Analysis of derivative control based virtual inertia in multi-area high-voltage direct current interconnected power systems. IET Gener. Transm. Distrib. 10(6), 1458–1469 (2016)
37. Liu, Z., et al.: Improved power flow control strategy of the hybrid AC/DC microgrid based on VSM. IET Gener. Transm. Distrib. 13(1), 81–91 (2019)
38. Li, Y., et al.: Novel grid-forming control of PMSG-based wind turbine for integrating weak AC grid without sacrificing maximum power point tracking. IET Gener. Transm. Distrib. 15(10), 1613–1625 (2021)
39. Walve, K.: Nordic32A—a Cigré test system for simulation of transient stability and long term dynamics. Technical Report, Svenska Kraftnät, Vällingy (1993)
40. Strunz, K., et al.: Benchmark systems for network integration of renewable and distributed energy resources. CIGRE, Technical Report (April, 2014)
41. Lai, N.B., et al.: External inertia emulation controller for grid-following power converter. IEEE Trans. Ind. Appl. 57(6), 6568–6576 (2021)
42. Xu, C., et al.: Transient stability analysis and enhancement of grid-forming and grid-following converters. IEEE J. Emerg. Sel. Top. Ind. Electron. 5(4), 1–14 (2024)
43. Yi, X., et al.: Transient synchronization stability analysis and enhancement of paralleled converters considering different current injection strategies. IEEE Trans. Sustainable Energy 13(4), 1957–1968 (2022)
44. Domínguez-García, J.L., Gomis-Bellmunt, O., Bianchi, F.D., Sumper, A.,: Power oscillation damping supported by wind power: a review. Renewable Sustainable Energy Rev. 16(7), 4994–5006 (2012)
45. Jankovic, N., Roldán-Pérez, J., Prodanovic, M., Rouco, L.,: Centralised multimode power oscillation damping controller for photovoltaic plants with communication delay compensation. IEEE Trans. Energy Convers. 39(1), 311–321 (2024)
46. Renedo, J., Garcia-Cerrada, A., Rouco, L., Sigrist, L.,: Coordinated design of supplementary controllers in VSC-HVDC multi-terminal systems to damp electromechanical oscillations. IEEE Trans. Power Syst. 36(1), 712–721 (2021)

How to cite this article: Paniagua, J., Unamuno, E., Barrena, J.A.: Virtual power line control for interlinking converters on AC, DC and hybrid grid links. IET Gener. Transm. Distrib. 19, e70021 (2025). https://doi.org/10.1049/gtd2.70021